Low-chromophore lignin isolation from natural biomass

Jinyuan Cheng[a,b], Chen Huang[a,b,*], Yunni Zhan[a], Xuelian Zhou[a], Xuze Liu[a], Tingjun Chen[a], Caoxing Huang[b], Chang Geun Yoo[f], Xianzhi Meng[c], Guigan Fang[a,* b], Arthur J. Ragauskas[c,d,e,*]

[a]Institute of Chemical Industry of Forest Products, Chinese Academy of Forestry, Jiangsu Province Key Laboratory of Biomass Energy and Materials, Nanjing 210042; [b]Co-Innovation Center for Efficient Processing and Utilization of Forest Resources, Nanjing Forestry University, Nanjing 210037, China; [c]Department of Chemical and Biomolecular Engineering, University of Tennessee Knoxville, Knoxville, TN 37996, USA; [d]Department of Forestry, Wildlife, and Fisheries, Center for Renewable Carbon, The University of Tennessee Institute of Agriculture, Knoxville, TN 37996, USA; [e]Joint Institute for Biological Science, Biosciences Division, Oak Ridge National Laboratory, Oak Ridge, TN 37831, USA; and [f]Department of Paper and Bioprocess Engineering, State University of New York College of Environmental Science and Forestry, Syracuse, New York 13210-2781, United States.

When attempting to obtain light-colored lignin from lignocellulosic biomass or even industrial lignin, the available options focusing on chemical or morphological modification suffer from low performance, high cost, and lack of availability at the required scales. In this study, we combined chemical structure stabilization and morphology regulation using a polyhydric-alcohol-based deep eutectic solvent (PA-DES) to directly obtain light-colored lignin analogous to cellulolytic enzyme lignin (CEL), which simultaneously yielded digestible cellulose-rich residues with a subsequent glucan enzymatic hydrolysis of 99.47%. The isolated lignin possessed a high recovery yield (97.36%), regular micro-spherical morphology, enriched β-ether linkage of 58/100Ar, low phenolic hydroxyl content of 1.25 mmol g^{-1}, minimal carbonyl content of 0.70 mmol g^{-1}, and less condensed structures, thus yielding a lower content of chromophores. These lignins showed excellent sunscreen effects, which could enhance the commercial SPF 15 sunscreen to SPF 40 with only a 5% addition. The light-colored lignin formation mechanism during PA-DES fractionation was revealed by 2D HSQC NMR, ^{31}P NMR, ^{19}F NMR, and GPC analyses. This study can provide essential guidance for the scale-up production of light-colored lignin and obtaining near-whole digestible cellulose for further saccharification.

In the context of carbon neutrality, there is an urgent need to explore and develop renewable and sustainable resources to reduce the growing energy consumption and environmental problems caused by over-reliance on fossil fuels[1]. Lignocellulose, which consists of cellulose (30-50%), hemicellulose (10-35%), and lignin (15-35%), is the most abundant and sustainable green carbon resource on Earth[2]. Utilization of lignocellulosic biomass is a feasible approach for achieving carbon neutrality. However, the naturally recalcitrant structure and stubborn lignin-carbohydrate complex (LCC) frameworks make it difficult to valorize lignocellulose[3]. Thus, fractionation of biomass is an essential prerequisite for obtaining high value-added chemicals and products. Conventionally, carbohydrate-centered processes focusing on (hemi)cellulose utilization are the mainstream, for example, dilute sulfuric acid, kraft, or sulfite processes, whereas in these methods, lignin is irreversibly degraded or converted to a condensed product with a dark color, which makes it difficult to utilized[4]. Recently, methods such as organic acid[5] and organosolv fractionation[6] have been widely investigated for the pretreatment of biomass and isolation of lignin for high-value-added upgrading. Although these fractionation strategies can extract lignin with a relatively high reactivity, the recovered lignin still features a dark color[7]. The undesired dark color of isolated lignin greatly constrains its high-value applications, such as dye dispersity and sunscreen additives. Therefore, it is important to whiten lignin, especially during its isolation process, to an acceptable color to expand its valorization.

Deep eutectic solvents (DES) consist of one hydrogen bond acceptor (HBD) and at least one hydrogen bond donor (HBA) and possess a lower melting point than that of each constituent[8]. Compared with ionic liquids, they have outstanding properties such as environmental friendliness, low cost, biodegradability, and non-flammability, and possess excellent dissociation of lignin and hemicellulose while preserving cellulose during lignocellulose fractionation[9,10]. However, previous DES fractionation processes have paid too much attention to the isolation of lignin and hemicellulose to enhance cellulose accessibility, while neglecting the lignin quality and its upgrading potential, with a common dark color issue. For example, Shen et al. established a ChCl/lactic acid system for *Eucalyptus* fractionation, which obtained a 94.3% glucan saccharification yield, while the recovered lignin was greatly transformed, accompanied by severe condensation reactions[11]. Another study using ChCl/*p*-hydroxybenzoic acid for poplar fractionation yielded a glucose yield of over 90%, but with severe degradation and condensation reactions for the recovered lignin[12]. Excessive degradation and condensation of the isolated lignin greatly reduces the reactivity of lignin and darkens the color of lignin, which limits lignin valorization in dye dispersity or sunscreen additives. Fortunately, polyol as the HBD in DES for lignocellulose fractionation has been reported in our previous work[13], which could protect lignin from further degradation and condensation, thus generating a less condensed lignin with a light color. However, the mechanism for the color reduction of the extracted lignin in terms of morphology mediation and structural stabilization

has not yet been investigated.

Natural lignin is light brown and has a strong UV-shielding property, which is considered the ideal choice for sunscreen production[14]. However, during lignin isolation, especially under harsh conditions (*e.g.*, strong acidity, high temperature, and long fractionation time), various chromophore groups are induced by the formation of carbon-carbon double bonds conjugated with aromatic rings, quinone methides, quinones, chalcone structures, or metal complexes with catechol structures darken lignin[15–17]. Numerous strategies have been proposed to decrease chromophore groups and whiten lignin by modifying its morphology and chemical structure. For example, ground lignin with tiny particles is obviously lighted by more than threefold compared with untreated lignin[18]. In addition, significant color fading of Kraft lignin was obtained through the rearrangement of chromophores by self-assembly into colloidal spheres[16]. In another study, acetylation treatment was used to protect the phenolic hydroxyl groups to change the color of alkaline lignin from black to brown[17]. In brief, previous processes to obtain light-colored lignin mainly relied on the decoloration of commercial lignin by complicated processes, whereas the direct output of light-colored lignin by morphology mediation and structural stabilization from lignocellulose biomass has not been reported.

In this study, light-colored lignin was obtained by the PA-DES pretreatment of bamboo using choline chloride (ChCl)/polyhydric alcohol (PA)/$AlCl_3$ under mild conditions (110 °C for 1 h). This study unveiled the formation mechanism of light-colored lignin through morphology regulation and chemical structure stabilization, which will provide promising guidance for methods and mechanisms to obtain high-yield and light-colored lignin while enhancing cellulose saccharification for the high-value upgrading of lignocellulose.

Results and Discussions

Selective Degradation of Lignin and Hemicellulose. The ChCl/glycerol/$AlCl_3$ (GLDES) system was first used to determine the optimal pretreatment conditions for PA-DES. As shown in Fig. 1A, the solid yield significantly decreased from 73.28% to 58.63% as the temperature increased from 100 °C to 110 °C, while it remained nearly constant as the temperature reached 120 °C. For each component, xylan removal increased from 62.98% to 86.40%, and lignin removal also showed the same trend from 22.86% to 70.74% when the pretreatment temperature increased from 100 to 120 °C. In the case of glucan, its recovery remained constant (94.15%-95.32%) despite the increase in temperature, implying that glucan was very stable during GLDES treatment. Considering the satisfactory removal of lignin (66.20%) and xylan (80.23%), and the near-complete preservation of glucan (95.32%) at 110 °C, this temperature was chosen for the investigation of other PA-DES pretreatments.

ChCl/ethylene glycol/$AlCl_3$ (EGDES) and ChCl/butanediol/$AlCl_3$ (BDDES) were studied using the same procedures and were compared with GLDES. The compositional analyses of the different PA-DESs systems are shown in Fig. 1B. The solid yield of EGDES was 67.81%, and that of BDDES was 59.29 %, slightly higher than that of GLDES, but still showed significant fractionation performance. Furthermore, xylan removal was 65.97-80.23% in different PA-DESs treatment

systems, in which EGDES showed the lowest xylan removal, while GLDES obtained the highest removal. The excellent hemicellulose removal in GLDES might be ascribed to the stronger H-bond interaction, because GL with three OHs has a higher H-bond donating ability[19]. In addition, lignin removal also depended on the PA type, which increased from 55.07% (EGDES) to 66.20% (GLDES) but reached the highest value of 70.63% for BDDES. This trend indicates that the H-bond quantity alone cannot determine the pretreatment performance; other factors, such as the inherent solvent properties, also have a significant effect.

For cellulose, the glucan recovery yields could reach 95.32-99.04% throughout the different PA-DES systems, suggesting that all the PA-DES fractionations could preserve the cellulose. The pretreated solids exhibited excellent enzymatic saccharification (*SI Appendix*, Fig. S1). Raw bamboo had a limited saccharification yield, with only 12.63% glucan and 1.74% xylyan saccharification yields (*SI Appendix*, Fig. S1). After EGDES pretreatment, the glucan and xylan saccharification yields dramatically increased to 86.82% and 95.78%, respectively, which were enhanced by 6.87 and 50.05 times compared to the raw bamboo, respectively. Both GLDES and BDDES led to over 90% glucan and xylan saccharification yields, outperforming other conventional DESs such as ChCl/formic acid[20], ChCl/oxalic acid[21], and ChCl/*p*-hydroxybenzoic acid[12]. These results implied that our PA-DESs could easily achieve satisfactory carbohydrate conversion through enzymatic hydrolysis.

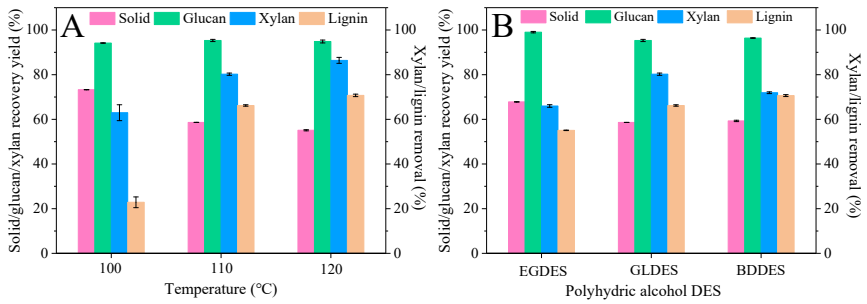

Fig. 1. Component analysis of the pretreatment under different temperatures of the GLDES system (A) and different PA-DESs systems (B) at 110 °C.

Lignin Recovery and Carbohydrate Analysis. After DES fractionation, lignin recovery yield and its components were determined (*SI Appendix*, Table. S1). It can be seen that the isolated lignin of PA-DES showed near-complete recovery (94.62-97.36%), which is higher than most reported fractionation systems such as alkaline[22] and organosolv processes[6,23], indicating that our proposed PA-DESs fractionation system could easily regenerate lignin from lignocellulose. We also performed the pretreatment using traditional ChCl/lactic acid (LADES) and ChCl/oxalic acid (OADES), the lignin recovery yields in these methods were only 79.65% and 75.68%, respectively. This is likely because lignin in conventional acid DES pretreatment usually suffers from serious degradation and condensation that precipitate back onto the substrate surface. In contrast, PA-DES partially protected the lignin degradation

products from being condensed, which increased its solubility in DES and facilitated its recovery.

Considering the high lignin recovery yields and significant xylan removal during the fractionation processes, monosaccharides may be present in the recovered lignin, which is detrimental to further valorization. Thus, component analysis was conducted to analyze its purity. Surprisingly, only trace monosaccharides were tested in the regenerated lignin (less than 0.11% glucan and 0.16% xylan), implying the high purity of the recovered lignin. The high-purity lignins recovered from our PA-DESs were favorable for further valorization.

Color appearance and morphological analysis. The appearance of the recovered lignins is shown in Fig. 2A; lignin extracted through the PA-DES systems exhibited a light brown color, which was even whiter than that of the native CEL. In contrast, lignin isolated from organic acid-based DES (LADES and OADES) featured a dark brown color. The bulk density of the isolated lignins was macroscopically quantified. The lignins recovered from both the OADES and LADES systems have high bulk density of 0.58 and 0.55 g cm^{-1}, respectively (*SI Appendix*, Fig. S2). However, the bulk density of lignins recovered from the PA-DES fractionation system ranged from 0.24 to 0.28 g cm^{-1}), over 50% lower than that of the OADES and LADES, indicating their loosen macro-structure. Specifically, the visible color of the recovered lignins was negatively correlated with their bulk density, suggesting that a higher bulk density might have a tight structure and result in a dark color, as will be discussed later.

To quantify the differences in the color of the different recovered lignins, the lignin samples were further evaluated using L*a*b* values and brightness. As shown in Fig. 2B, the L*, a*, and b* values in the CEL were 69.32, 4.72, and 26.75, respectively. The lignins recovered from the PA-DESs had similar L*a*b* values, close to that of native CEL, which explains why our PA-DESs could yield light-colored lignin. In contrast, lignins from both organic acid-based DESs had extraordinarily lower L*a*b* values, especially L_{OADES}, which possessed L*a*b* values of 34.33, 3.61, and 10.71, respectively. For brightness, it is 22.39% ISO for native CEL. After traditional acidic OADES and LADES fractionation, lignin brightness decreased significantly to 5.59 and 7.69% ISO, respectively (Fig. 2C). Importantly, the lignin extracted from PA-DES had a higher brightness than that of the native CEL. Specifically, a brightness of 22.62% ISO and 25.91% ISO was observed for L_{BDDES} and L_{EGDES}, respectively. Furthermore, L_{GLDES} possessed the highest brightness of 29.84% ISO. These results suggest that our PA-DESs, especially the GLDES system, can isolate light-colored lignin whose brightness even exceeds that of native lignin. Lignin color is generally related to chromophore content and micromorphology. Therefore, the mechanism of our PA-DESs recovered lignin with a light color was revealed by the micromorphology and chemical structure, which will be illustrated later.

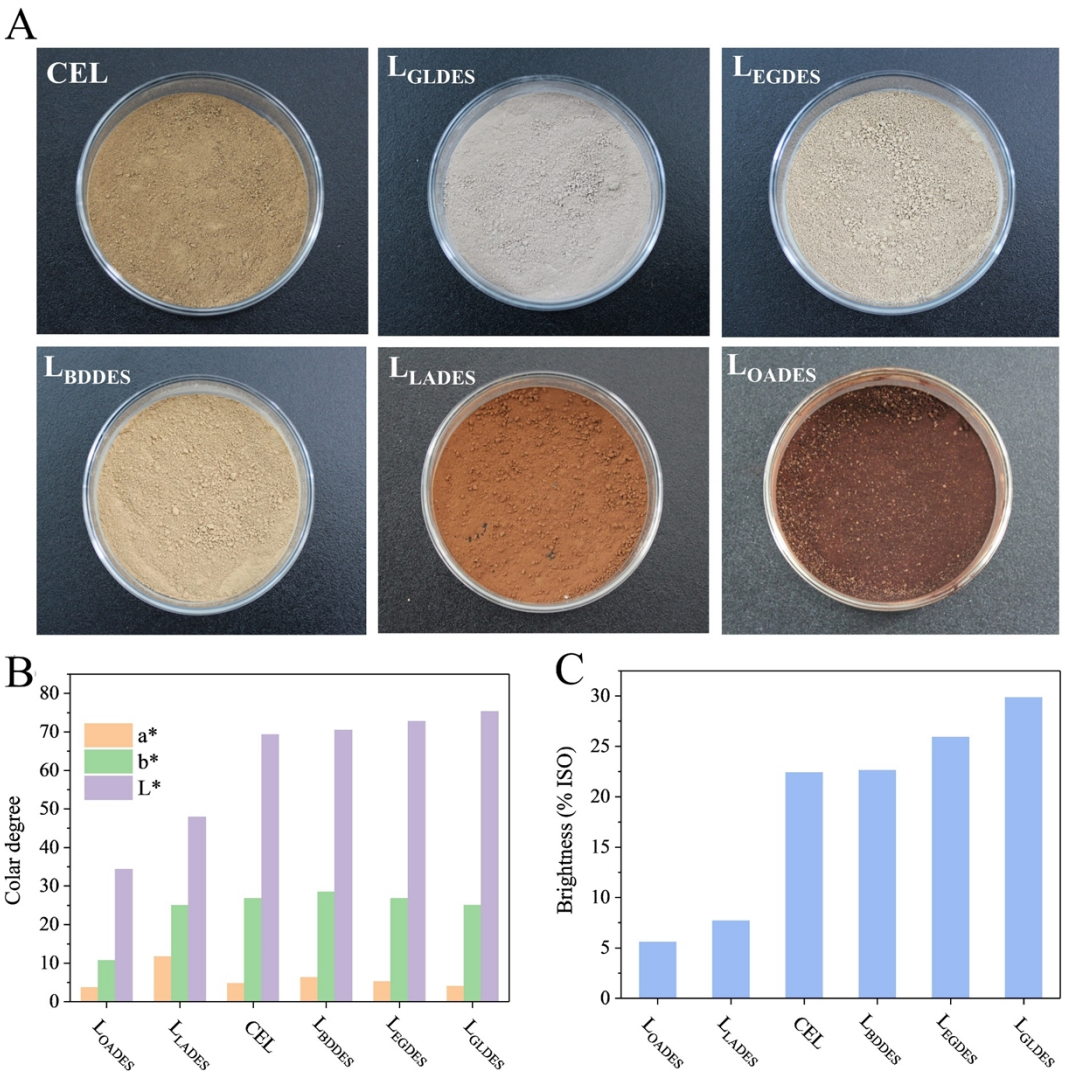

Fig. 2. Digital photographs of the recovered lignins (A), L*, a*, and b* values of the recovered lignins (B), and the brightness of the recovered lignins (C).

Micromorphology Analysis. The micromorphology of the lignins obtained from the PA-DESs fractionation systems was determined using FE-SEM. As shown in Fig. 3, all lignins featured a uniform spherical shape and were termed lignin microparticles (LMPs). The average size of the LMPs varied from 550 to 3254 nm, with a narrow PDI of 0.30-0.40 depending on the type of PA-DES. Specifically, LMPs isolated by the GLDES system had the smallest average size (550 nm) and narrowest PDI (0.30), corresponding to the lightest color. The other two LMPs had much larger average sizes of 1080 nm (EGDES) and 3254 nm (BDDES). This result indicated that the PA-DES system could directly generate uniform LMPs with different PA as the HBD, which probably resulted from the structural modification by PA (*e.g.*, connecting bonds, molecular weight, and hydroxyl groups) during the fractionation process. Interestingly, it was found that the color degree (L*a*b* and brightness) of the LMPs was negatively correlated with the size of the LMPs, in which smaller LMPs have a lighter color. In general, LMPs with small average sizes can increase the specific surface area and simultaneously enhance the interval spaces, resulting in a low bulk

density. In this vein, it is likely that lignin contains similar amounts of chromophores with a low bulk density, which can decrease the concentration of chromophores at the macroscopic scale, thus resulting in the light color of lignin[18].

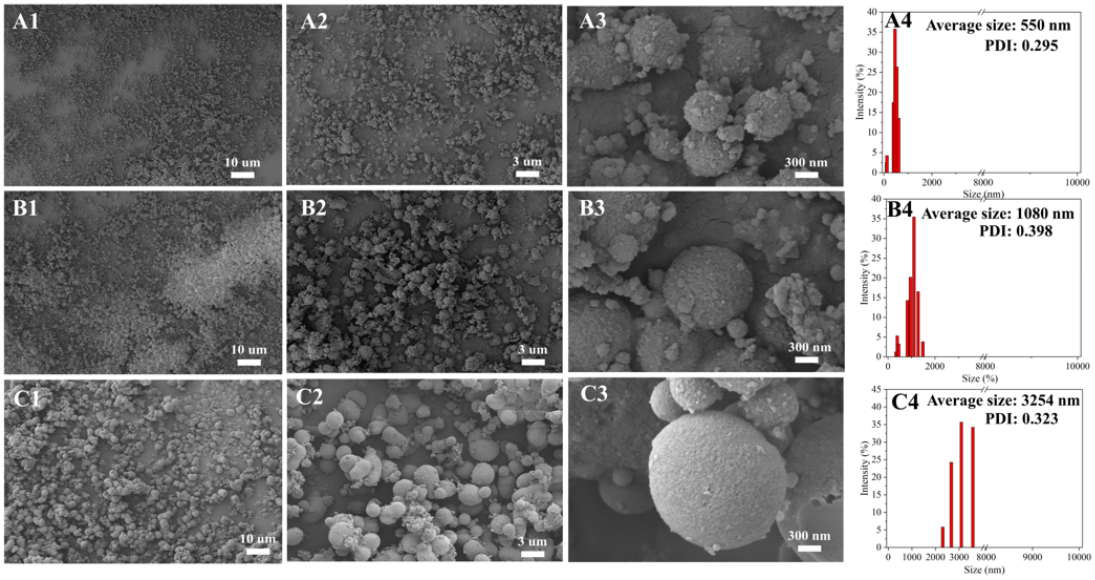

Fig. 3. SEM images of isolated LMPs of L_{GLDES} (A1-A3), L_{EGDES} (B1-B3) and L_{BDDES} (C1-C3) and their size distributions (A4-C4).

In contrast, the CEL and lignins recovered from the organic acid-based DES adopting the same procedures as the polyol-based DES featured irregular bulk-like shapes, which were wrapped by unordered lignin debris (Fig. 4). This result suggests that our PA-DESs possess special functionalities for directly extracting lignin from lignocellulose and upgrading it into uniform LMPs. Importantly, the bulk-like shape of the lignin isolated from the organic acid-based DES was also associated with its dark color because of its low specific surface area and interval spaces compared with those of the LMPs.

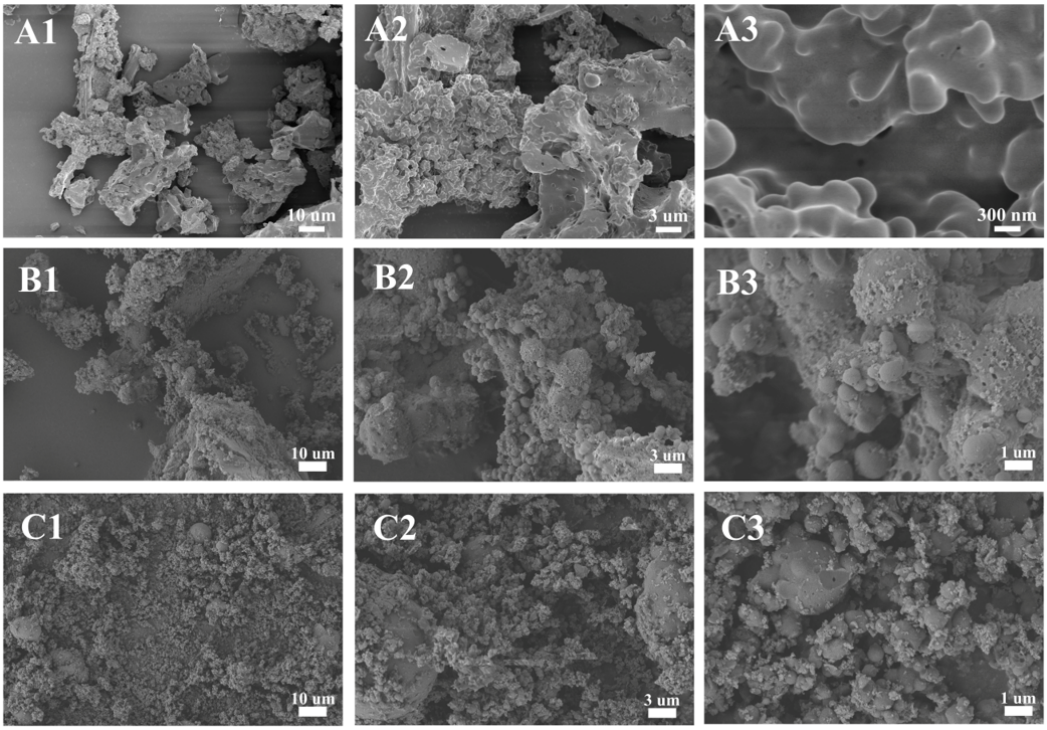

Fig. 4. Morphology of CEL (A1-A3) and lignins isolated from organic acid-based DES systems of LADES (B1-B3) and OADES (C1-C3).

Structural Analysis of the Isolated Lignins. The molecular weights (M_w and M_n) and polydispersity indices (PDI) are shown in Fig. 5. For CEL, the M_w was 12322 g mol^{-1}, and it significantly decreased after all the pretreatments, implying the existence of lignin depolymerization during fractionation. Specifically, PA-DES generated lignin with a high M_w in the order of L_{GLDES}>L_{EGDES}>L_{BDDES}. In contrast, lignin isolated from the organic acid-based DES had a much lower M_w of 3906 and 3026 g mol^{-1}, which is significantly lower than that of lignin isolated from the PA-DES system. It is well known that the molecular weight of lignin is positively correlated with the content of aryl ether linkages, suggesting that our PA-DES has the unique ability to preserve the lignin structure. Notably, the color degree of lignin represented by L*a*b* and brightness is also positively related to its M_w, which implies that high-M_w lignin possesses fewer chromophores. In addition, the lignin recovery yield was found to be positively correlated with M_w because intact lignin can be easily recovered, as reported in previous studies[24,25]. In addition, The PDI of lignin significantly decreased with decreasing M_w.

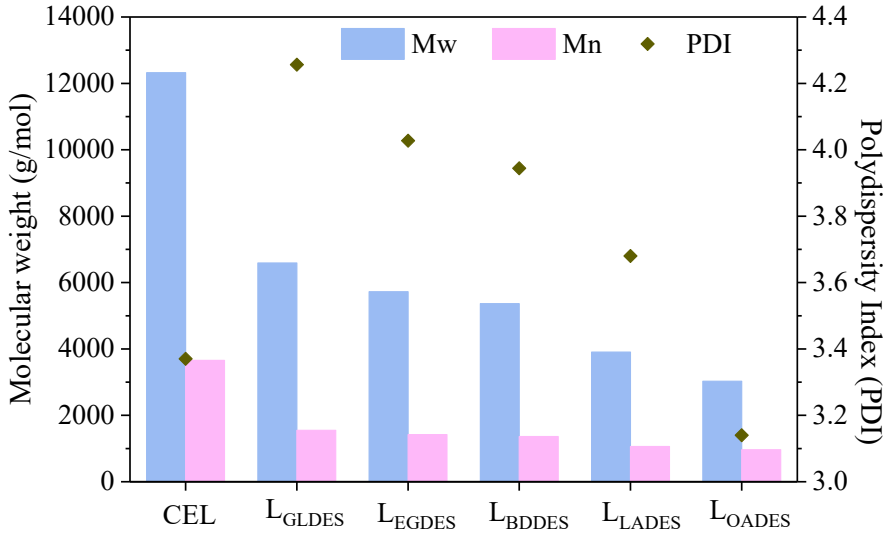

Fig. 5. Molecular weight determination of CEL and the isolated lignins.

To analyze the variation of the lignin structure in the DES pretreatment, 2D-HSQC NMR was conducted, and CEL was used as a contrast. The HSQC spectrograms of the side-chain and aromatic regions of the CEL and the recovered lignins are shown in Fig. 6 and 7, and the reaction mechanism of lignin during fractionation is also shown (Fig. 8). The main lignin cross-signal assignment of the spectrogram was labeled according to previous publications[26–28].

The aliphatic regions (Fig. 6) of the CEL of β-O-4 (A_α), β-β (B_α), and β-5 (C_α) exhibited strong signals at δ_C/δ_H 71.61/4.83, 84.72/4.64, and 86.85/5.40 ppm. Unambiguous signals relating to β-O-4 (A_β), β-β (B_β), and β-5 (C_β) were also observed at 86.1/4.05 (A_β for S) and 83.4/4.33 (A_β for G), 53.5/3.05, and 52.4/3.45 ppm, respectively. The γ-position of β-O-4 (Aγ), β-β (Bγ), and β-5 (Cγ) signals were centered at 59.5/3.69, 71.0/4.16-3.79, and 62.3/3.70 ppm, respectively. A signal belonging to γ-acetylated β-O-4 linkages (A′γ) was clearly recognized, implying that the LCC structure exists in bamboo. The quantification of CEL and the isolated lignins is shown in Table. 1. In CEL, the β-O-4 linkages' content was 59.19/100Ar, and it was greatly reduced after the PA-DESs fractionation, which ranged from 13.76 (LGLDES) to 9.36 (LEGDES) and 4.73/100Ar (L_{BDDES}), indicating that the β-O-4 linkages' content was greatly determined by the type of PA-DES. With the reduce of the signal of β-O-4 linkages, a strong signal at 80.05/4.49 ppm appeared, which was ascribed to the PA-functionalized β''-O-4 (A''_α) through α-OH etherification in the lignin side chains (see the red circles in Fig. 6). Notably, this functionalization resulting from PA could significantly stabilize the β-O-4 linkages in lignin, protect it from degradation during fractionation, and efficiently inhibit lignin repolymerization reactions[13,29]. This functionalization made the total β-O-4 linkages (A_α and A''_α) maintained at as high as 52.51 (L_{EGDES})-58.01/100Ar (L_{GLDES}), which equivalently account for 88.71-98.01% of the CEL. It is widely acknowledged that β-ether cleavage is accompanied by the generation of potential chromophores of phenolic hydroxyls, which can be readily converted into ketones, aldehyde and quinoid structure[30]. The existence of these structures is regarded as one of the dominant

reasons for the darkening of lignin[31]. Notably, lignin protection by PA could significantly hinder the formation of phenol hydroxyl, thus greatly restricting the formation of phenol hydroxyl and avoiding the dark color of lignin. The other C-C linkages, including β-β and β-5, slightly decreased after PA-DES fractionation, indicating that the C-C linkages were stable during the treatment (*SI Appendix,* Table. S2). Moreover, the β-ether content in the recovered L_{LADES} greatly decreased to 28.49/100Ar, and was absent in L_{OADES}. As for the C-C linkages, the β-β and β-5 in L_{LADES} decreased to 2.46 and 4.21/100Ar, respectively, and both of them finally disappeared in L_{OADES} (*SI Appendix*, Table. S2). These results implied that β-ether and other C-C linkages could be easily cleaved without PA protection. Significant β-ether cleavage greatly facilitated the generation of potential conjugated chromophores of aldehyde-containing monomers and Hibbert's ketone, which could be converted into conjugated chromophores by aldol condensation[32], thus darkening the color of lignin.

To clarify lignin functionalization, a mechanism was proposed, as shown in Fig. 8. In common acid fractionation systems, a carbocation at the α-position of lignin side-chains can be easily formed by H^+ attack (process A in Fig. 8), which partially results in condensation reactions with the adjacent lignin debris[33]. Furthermore, β-ether acidolysis occurs mainly *via* two pathways: one leads to the cleavage of C_β-C_γ with aldehyde-containing lignin debris and formaldehyde (C_2 pathway of F), whereas the other forms Hibbert's ketone lignin debris (C_3 pathway of D) under acidic conditions. Both types of carbonyl monomers may undergo further aldol condensation (pathway H) or condensation with C_2 or C_6 on the lignin aromatic rings[32]. During these β-ether cleavage and condensation reactions, the formation of the conjugated C=O and C=C structures (products 8 and 9 in Fig. 8) might be the pivotal reason for the darkening of lignin in most acid fractionation processes, including the contrastive systems of LADES and OADES in this study. In the PADES process, PA can readily graft onto the α-position of the carbocation intermediate (pathway C), thus significantly hindering the cleavage and condensation reactions of the β-ethers and leading to an intact lignin structure with low chromophores, such as CEL. Although minor β-ether of lignin might undergo acid acidolysis of C_2 and C_3 during PA-DES fractionation, PA (*e.g.,* EG) could also stabilize the acidolysis products or inherent carbonyl groups through acetal protection (pathways E and G, Fig. 8), thus quenching the potential chromophoric carbonyl groups. Overall, the significant protection induced by PA could result in an intact lignin structure, which has almost no chromophore formation during fractionation, thus leading to light-colored lignin.

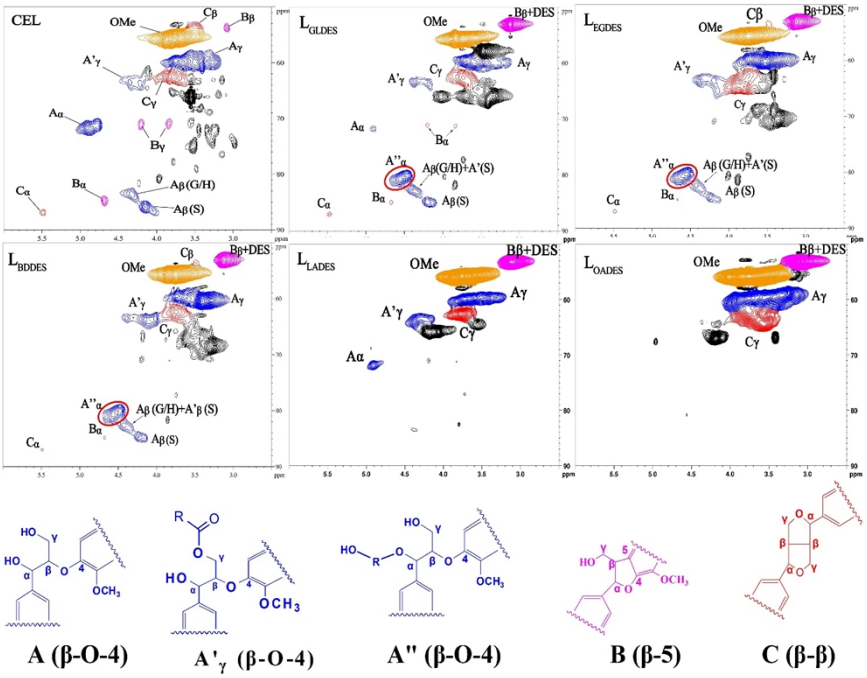

Fig. 6. Side-chain regions of CEL and the isolated lignin fractions.

In the aromatic regions (Fig. 7), signals of the guaiacyl (G), syringyl (S), oxidized syringyl (S'), and *p*-hydroxyphenyl (H) units were clearly observed in the CEL. In addition, ferulate (FA) and *p*-coumarate (PCE) signals were clearly identified. The cross peaks of $S_{2,6}$ and $S'_{2/6}$ were located at δ_C/δ_H 104.0/ 6.72 and 106.3/7.21 ppm. The signals ascribing to guaiacyl (G) were at 111.0/6.97 ppm (G_2), 114.8/6.69 ppm (G_5), and 119.1/6.81 ppm (G_6). The *p*-hydroxyphenyl (H) signal was located at δ_C/δ_H 127.9/7.19 ppm ($H_{2,6}$). After PA-DES fractionation, the $S_{2/6}$ signals showed no distinct shifts. Specifically, only a small amount of condensed S units was found throughout the fractionation, ranging from 7.82/100Ar (L_{GLDES}) to 9.32/100Ar (L_{BDDES}). It was even negligible throughout the PA-DES pretreatment for the condensed G units (1.52-2.58/100Ar). The small amounts of condensation reactions suggested that our PA-DES could preserve the lignin structure well, thus obtaining a light-colored lignin similar to CEL. The S/G ratio increased slightly from 0.95 to 1.31, suggesting that G units were easily transformed during the treatment. In addition, the H units decreased after PA-DES fractionation. As for the FA content, representing the variation of LCC linkages, it disappeared after PA-DES fractionation, while the PCE remained nearly constant (*SI Appendix,* Table. S2). These results may be due to significant hemicellulose degradation during pretreatment. In contrast, L_{LADES} also had low amounts of condensed G (2.51/100Ar) and S (8.28/100Ar), which might be ascribed to limited lignin degradation (only 34.56% lignin removal) under mild fractionation conditions (110 °C, 3 h). When fractionation occurred in a relatively harsh OADES system, the condensed S units dramatically increased to 24.72/100Ar, whereas the G units completely condensed (43.56/100Ar). Condensed lignin containing conjugated C=O and C=C structures with phenolics might be mainly responsible for the dark color of lignin. In addition, the H unit content of the L_{OADES}

increased significantly, while the PCE decreased significantly (*SI Appendix*, Table. S2). This result might have resulted from the PCE transformation into H units, indicating that the lignin structure changed significantly during fractionation.

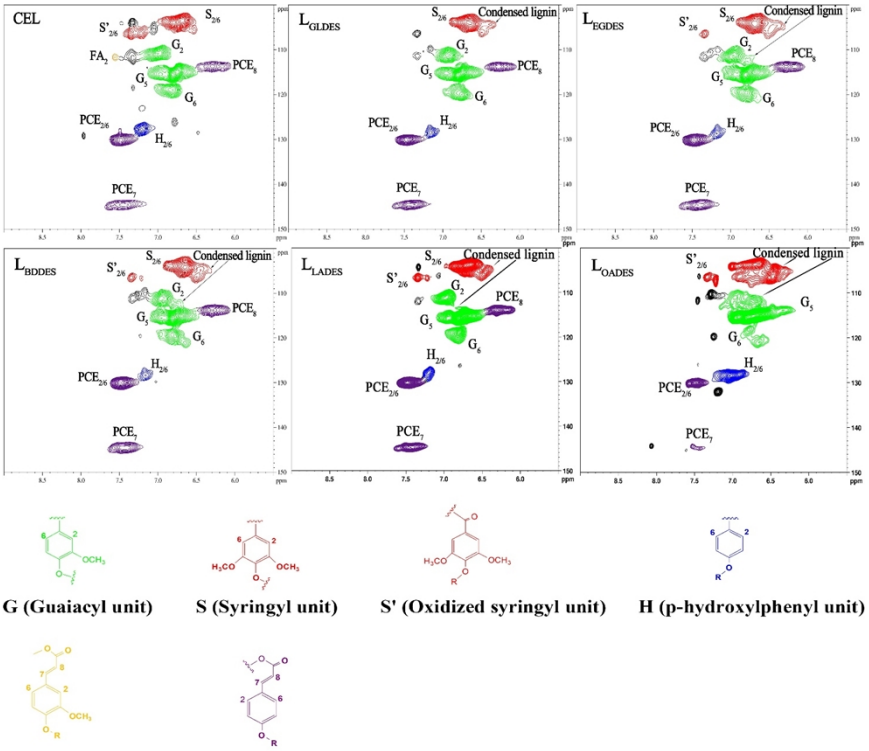

Fig. 7. Aromatic regions in the 2D HSQC NMR spectrograms of CEL and isolated lignins.

Table 1. Quantification of CEL and isolated lignins (per 100 Ar) by HSQC NMR

Sample	Lignin removal (%)	S (%)		G (%)		S/G	β-O-4 (%)	β''-O-4 (%)	Total β-O-4 (%)
		Total	Condensed	Total	Condensed				
CEL	-	43.39	0	45.82	-	0.95	59.19	0	59.19
L_{EGDES}	55.07	49.23	8.83	43.98	3.20	1.12	9.36	43.15	52.51
L_{GLDES}	66.20	48.42	7.82	47.70	1.52	1.10	13.76	44.25	58.01
L_{BDDES}	70.63	53.52	9.32	40.81	2.58	1.31	4.73	48.52	53.25
L_{LADES}	34.56	50.92	8.28	41.71	2.51	1.22	28.49	0	28.49
L_{OADES}	42.32	38.77	24.72	43.56	43.56	0.89	0	0	0

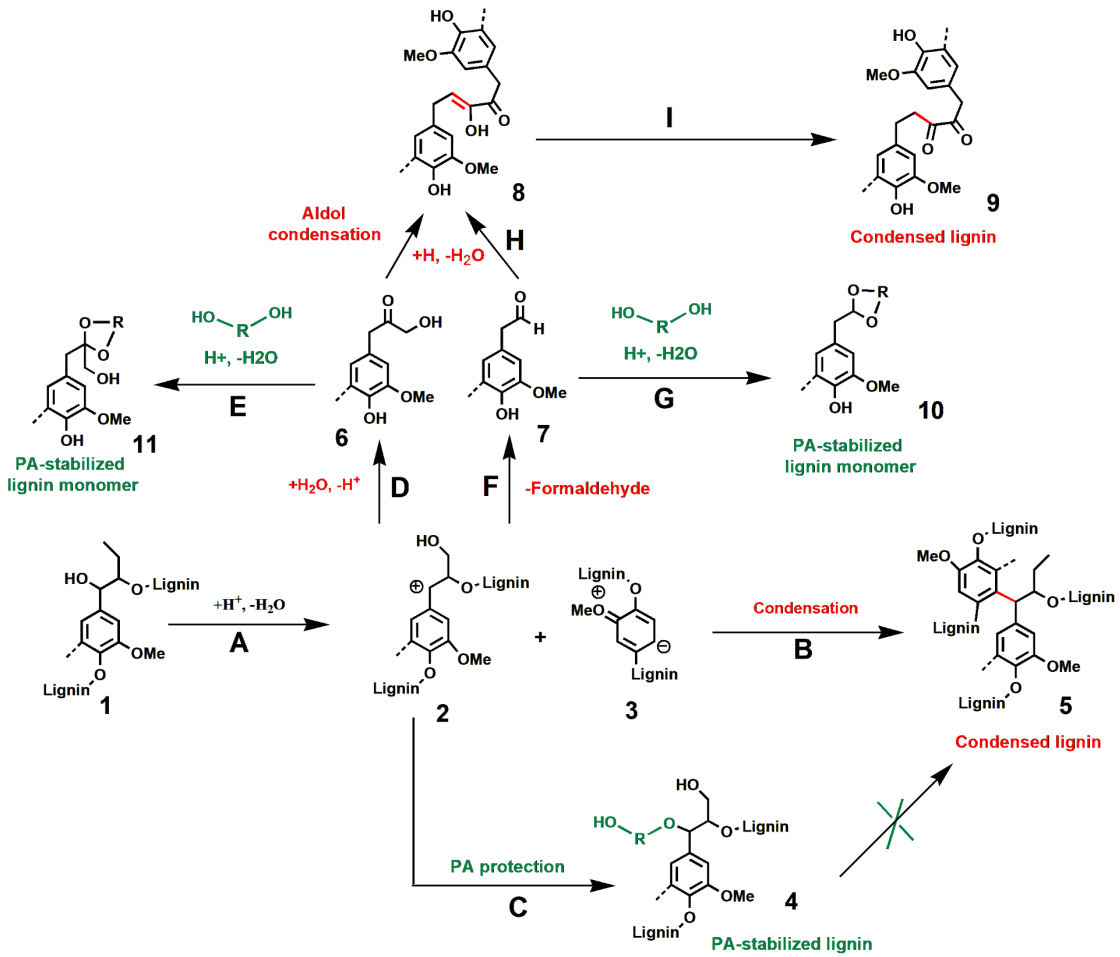

Fig. 8. Mechanisms of lignin degradation and PA stabilization.

The OH content, including aliphatic, phenolic, C_5 substituted (syringyl and other types of condensed 5-substituted), and carboxylic acid, was quantified by lignin phosphorylation followed by ^{31}P NMR. As illustrated in Fig. 9A, the aliphatic OH content in CEL was 3.61 mmol g^{-1}, accounting for 72.17% of the total OH groups. After PA-DES fractionation, it slightly decreased and ranged from 2.69 (L_{BDDES}) to 2.95 mmol g^{-1} (L_{GLDES}), but was still predominant in the total OH contents (66.33%-67.17%). In addition, the phenolic OH content in CEL was 1.18 mmol/g, accounting for 23.61% of the total OH. After pretreatment, the total phenolic OH increased only negligibly and was maintained at ~1.25, suggesting that there was no extra generation of phenolic OH during our PA-DES fractionation. This result is also consistent with the 2D HSQC NMR results, implying that our PA-DES could significantly constrain the generation of potential chromophoric groups through PA etherification stabilization. On the contrary, the aliphatic OH in L_{LADES} and L_{OADES} is much lower than the lignin recovered from PA-DES, which is 1.38 and 0.94 mmol g^{-1}, respectively. However, the total phenolic OH of both L_{LADES} (1.86 mmol g^{-1}) and L_{OADES} (2.73 mmol g^{-1}) is much higher than PA-DES' lignin. These results imply that lignin isolation without PA protection in common organic acid DES will result in a great increase in the potential chromophore of phenolic OH with a substantial sacrifice of the β-O-4 ether bond. In addition, the C_5-condensed OH in these acidic

systems was far beyond that of the PA-DES system, suggesting severe condensation reactions during fractionation. The increased lignin condensation, including the possible aldol condensation of lignin debris containing the conjugated C=O and C=C structures, might be one of the main reasons for the enhancement of lignin color.

It is widely acknowledged that conjugate structures in lignin induce the color of lignin, whether yellow, brown, or dark. These groups mainly include conjugated phenolic-, furan- and quinone structures, as can be seen in Fig. 9C. Among the known chromophores in lignin, nearly all of them possess carbonyl groups; thus, we quantified the carbonyl groups including ketone, aldehyde, and quinone of the CEL and recovered lignins by ^{19}F NMR (Fig. 9B) to better explain the reason for the light-colored lignin. It can be seen that the ketone, aldehyde and quinone groups in CEL were 0.31, 0.25 and 0.74 mmol g^{-1}, respectively. After GL- and EGDES isolation, each of these groups reduced, in which the L_{GLDES} possessed the lowest carbonyl contents of 0.13 (ketone), 0.11 (aldehyde) and 0.47 mmol g^{-1} (quinone), with a total carbonyl content of 0.70 mmol g^{-1}, indicating our PA-DES could quench the inherent carbonyl chromophores during its isolation. For L_{BDDES}, the carbonyl groups were almost unchanged and very close to the CEL. In the case of the acid DES (LA- and OADES), the total carbonyl content of the dark-color lignins recovered from organic acid-based DES of L_{LADES} and L_{OADES} were 2.1 and 3.1 mmol g^{-1}, respectively, far beyond that of the lignins isolated from the PA-DES system. As expected (*SI Appendix*; Fig. S3), the brightness of lignins had a significant negative correlation with the carbonyl group content of ketones (R^2=0.94), aldehydes (R^2=0.92), quinones (R^2=0.84), and total carbonyl groups (R^2=0.90), suggesting that carbonyl-derived chromophores were the main reason for the dark color of lignin.

Overall, the carbonyl-conjugated chromophore groups generated by aldol condensation during the conventional process mainly contribute to the dark color of the isolated lignin. This study successfully hindered the cleavage of β-ethers and aldol condensation reactions *via* PA-grafting reactions to avoid the generation of chromophorous groups of phenolic conjugated C=O and C=C structures, as well as the potential chromophores of phenolic OH groups or quenching the inherent chromophores of natural lignin in lignocellulose, thus yielding a light-colored lignin. In contrast, dark-colored lignins isolated from the organic acid-based system without PA protection showed severe cleavage of β-O-4 linkages, lignin condensation, and increased carbonyl content, especially in the OADES system, generating more chromophore groups and resulting in darker lignins.

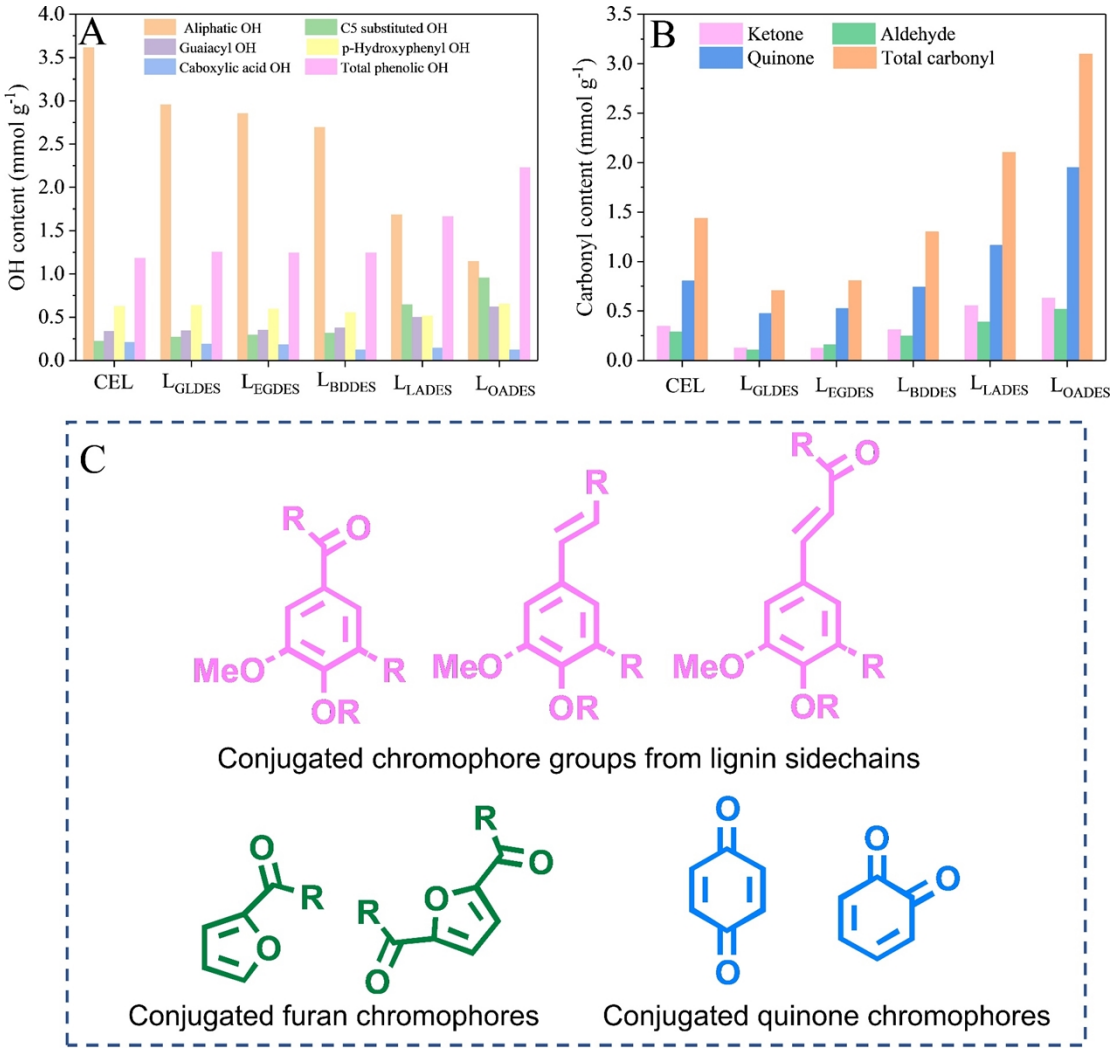

Fig. 9. Quantification of hydroxyl groups (A), carbonyl groups (B) of CEL, isolated lignins, and common chromophore groups in lignin (C).

UV-Protecting Properties of Light-Color LMPs. Considering the highest brightness of lignin recovered from the GLDES system, we chose L_{GLDES} for testing its application as a sunscreen agent. The light-colored lignin used in sunscreen was investigated by mixing it with pure cream or commercial SPF 15 sunscreen. As shown in Fig. 10A, the color of the prepared sunscreen with the naked eye slightly increased from white (1 wt% addition) to pale yellow (5 wt% addition) as the lignin content increased, while all these colors were close to our human skin, thus satisfying the makeup requirements. As for the sun protection properties (Fig. 10B and C), the pure cream had almost no absorbance in the UV (290-400 nm) areas, and its corresponding SPF was only 1.04. As lignin was introduced into the pure cream, the UV transmittance declined, and its corresponding SPF value was significantly enhanced. The transmittance decreased with increasing lignin loading. As the lignin content increased to 5%, the transmittance of the lignin sunscreen in the UVA (320-400 nm) and UVB (290-320 nm) areas was lower than 30%, and the SPF value was enhanced to 5.11 (Fig. 10C), ~5 times higher than that of pure cream, indicating that the light-

colored L_{GLDES} is a very good natural candidate for sunscreen.

Although it has excellent sunscreen performance in pure cream, it still cannot match the SPF values of the commercial sunscreen; therefore, we added L_{GLDES} to the commercial SPF 15 sunscreen to enhance its performance, such as commercial SPF 30 or SPF 50. For the commercial SPF 15 (Fig. 10D), the UV transmittance of partial regions of UVA (386-400) and UVB (290-297) was still over 10%, while it significantly declined as the lignin addition increased, and all of them decreased to < 8% with the addition of 5% lignin. As shown in Fig. 10E, the commercial SPF 15 sunscreen had an SPF value of 14.57, which dramatically enhanced to 25.72 (1% lignin addition) and exceeded common commercial SPF 30 after 3% lignin addition with SPF of 33.11. When the lignin content was further increased to 5%, the SPF value reached 42.91. In a previous study, the SPF value easily reached a plateau or even declined with increasing lignin addition because of its poor dispersity[34]. In this study, the SPF continually increased to as high as 42.91 with an increase in lignin content. This result might be due to the excellent dispersibility of the regular spherical microspheres in our L_{GLDES}.

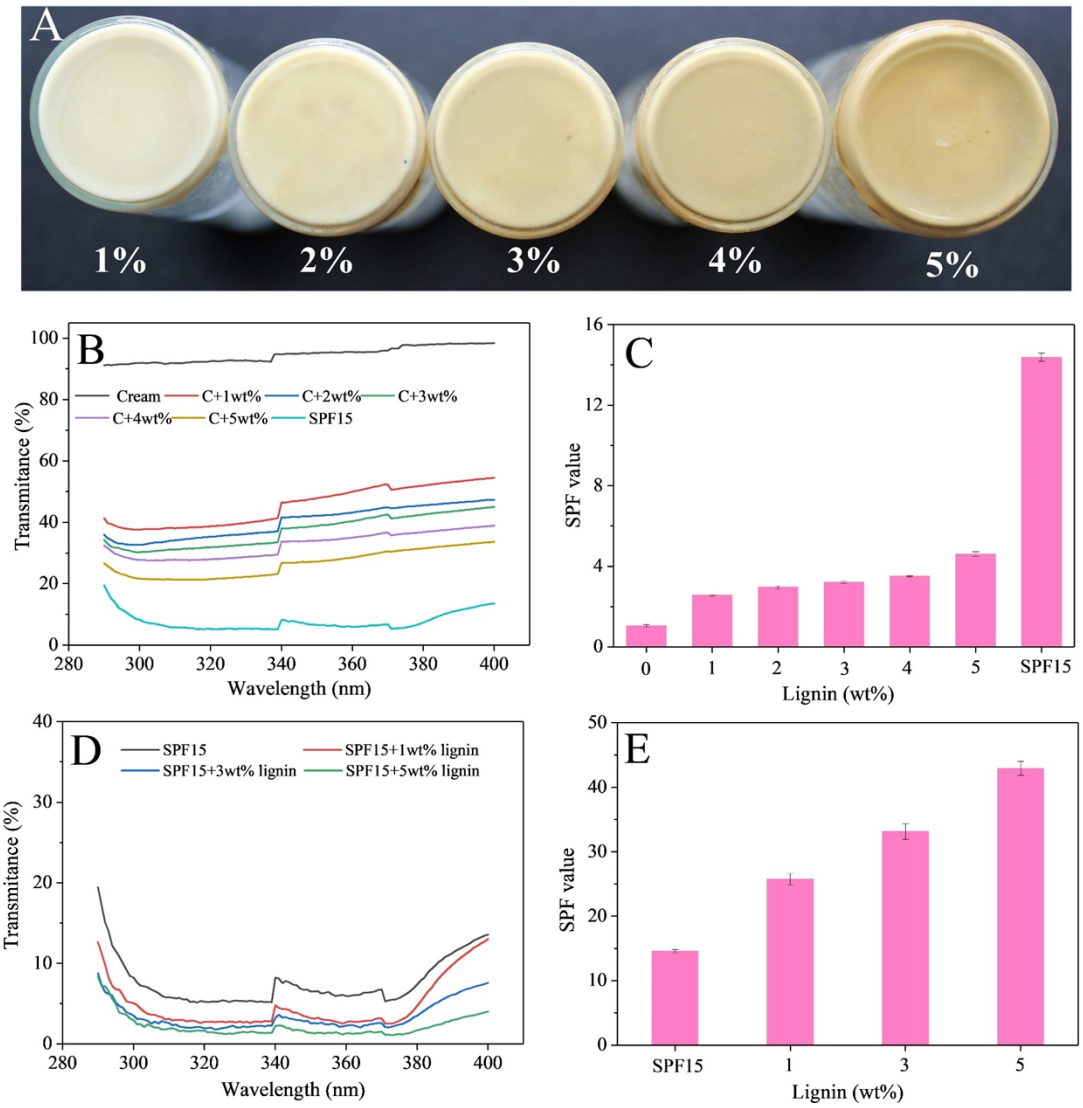

Fig. 10. Digital photographs of the pure cream with different LMPs additions (A); UV transmittance of the pure cream and lignin-added sunscreens with different amounts of lignin addition (B) and their corresponding SPF values (C); UV transmittance of the commercial SPF 15 sunscreen and lignin-added SPF 15 sunscreens with different lignin contents (D) and their corresponding SPF values (E).

Biorefining mass balance. Mass balance was performed using 1000 g of raw biomass as the starting feedstock using the GLDES system at the fractionation condition of 110 °C for 1 h. As shown in Fig. 11, 586.28 g cellulose-rich solid was recovered after the fractionation, which contained 391.77 g glucan, 25.27 g xylan and 107.75 g lignin. The subsequent enzymatic saccharification process yielded 433.12 g glucose and 28.72 g xylose which could be converted into fuels and chemicals. In addition, 205.15 g of lignin was isolated and 199.74 g of light-color lignin microspheres with a 97.36% lignin recovery yield were obtained using a simple antisolvent method, which possessed a conspicuous UV shielding performance for sunscreen production. In the fractionation liquor, 11.35 g xylose and 14.12 g furfural were quantified, which could also be isolated and converted into fuels and chemicals.

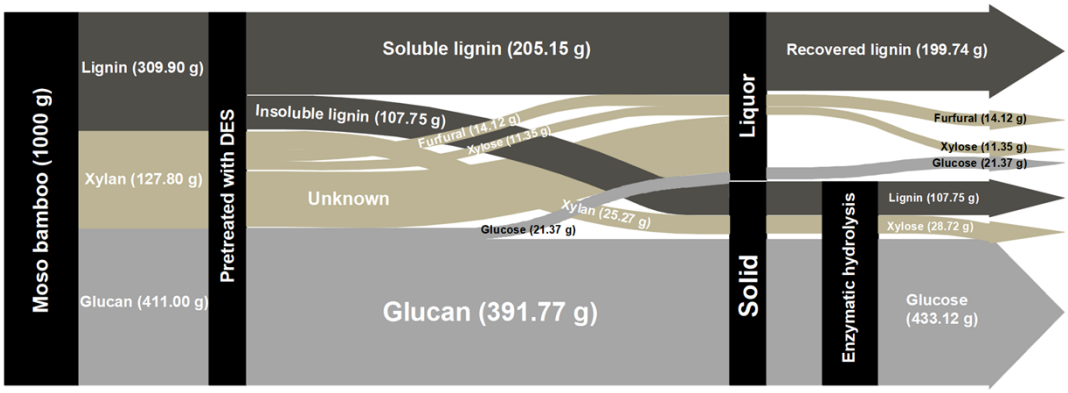

Fig. 11. Mass balance diagram of the GLDES fractionation system.

Conclusions

In this study, one-pot PA-DES fractionation using lignocellulose was proposed for directly obtaining light-colored lignin analogous to CEL. The recovered lignin possessed 29.84% ISO whiteness with a regular micro spherical morphology, high recovery yield (97.36%), enriched β-ether linkage of 58/100Ar, low phenolic hydroxyl content of 1.25 mmol g^{-1}, minimal C=O content of 0.70 mmol g^{-1} and less condensed structure. The mechanism for the generation of light-colored lignin was systematically analyzed. The recovered lignin showed excellent performance in sunscreen applications, which could easily enhance the sun protection factor of commercial SPF 15 to SPF 40 with the addition of 5% lignin. The recovered cellulose-rich residue obtained 99.47% enzymatic saccharification yield, which could be further converted into fuels. Overall, this study elucidated the mechanism for obtaining light-colored lignin while simultaneously enhancing the enzymatic saccharification yield, which could provide an essential reference for producing light-colored lignin and digestible cellulose.

Materials and methods

Materials. Bamboo (*Phyllostachys edulis*) harvested in Zhejiang Province (China) was processed into chips in a local pulping factory. After being received, the bamboo chips were washed and immersed in DI water overnight and then subjected to fibrillation using a twin-screw extruder. Finally, the fragmented feedstock was air-dried and transferred to a bag for further use. Cellulase (Cellic® CTec2, Novozymes) and xylanase (X2753-50 g) were obtained from Sigma-Aldrich (Shanghai, China). Pure NEVEA soft moisturizing cream (75 mL) and Curél SPF 15 sunscreen were purchased from Alibaba. Choline chloride (ChCl), ethylene glycol (EG), glycerol (GL), 1,4-butanediol (BD), $AlCl_3$, oxalic acid (OA), lactic acid (LA) and ethanol were purchased from Sinopharm Chemicals (Beijing, China).

DES Synthesis, Pretreatment, and LMPs Formation. DESs were synthesized in a three-neck flask by mixing ChCl, polyhydric alcohols (PA), and $AlCl_3$ at a molar ratio of 25:50:1 with constant stirring until a transparent and homogeneous liquid was formed at 90 °C. In addition, organic acid-based DES, including oxalic acid (OA)-and lactic acid (LA)-based DESs, were prepared by mixing ChCl and organic acids at a molar ratio of 1:2 using the same procedure. According to the variety of HBD, the DES systems were shortened to EGDES (ChCl/EG/$AlCl_3$), GLDES (ChCl/GL/$AlCl_3$), BDDES (ChCl/BD/$AlCl_3$), OADES (ChCl/OA), and LADES (ChCl/LA), respectively.

For the treatment process, 10 g of dry bamboo was blended with 100 g of DES at the target temperatures of 100-120 °C with constant stirring for 1 h. Notably, considering the poor lignin isolation of the LADES system[11], the LADES pretreatment was conducted for 3 h at 110 °C. At the end of each reaction, 300 mL of ethanol/water (1:1, v:v) was poured into the reactor to terminate the treatment, and the mixture was transferred into a beaker and magnetically stirred for 2 h. Next, the solid and liquid were separated by vacuum filtration, after which 200 mL of fresh ethanol solution was added to wash the solid thrice. The collected lignin-rich liquid was then evaporated to remove ethanol, and 500 mL of water was added to precipitate and recover the lignin. After washing with excess DI water to neutral pH, lignin was finally obtained by freeze-drying.

Enzymatic Saccharification. Enzymatic saccharification was performed in a 150 mL flask by adding substrates, cellulase (25 FPU per g-glucan), xylanase (150 U per g-xylan), acetate buffer, and DI water in a glass flask at a substrate concentration of 2.5%. The flasks were incubated in a shaker (50 °C, 150 rpm) for 72 h. At the end of the incubation, 1 mL of liquid was sampled, diluted, and analyzed by high-performance liquid chromatography (HPLC).

Characterization of the Lignin. The lignin recovery yield was analyzed according to the extracted lignin in the liquid, and the corresponding equation is as follows:

$$\text{Lignin yield (\%)} = \frac{\text{Lignin recovered from the treatment liquid (g)}}{\text{Total removed lignin from the initial substrate (g)}} \times 100\%$$

Sugar analysis of the recovered lignin was conducted using the NREL (National Renewable Energy Laboratory) protocol as previously described[35]. Cellulolytic enzyme lignin (CEL) was obtained following successive enzymatic digestibility and dioxane extraction process[25].

The lignin bulk density was tested in a 5 mL cylinder according to a previous publication[18]. The bulk density was obtained based on the weight of the lignin and the recorded volume. The color of the recovered lignin was analyzed using digital photographs, and its brightness was quantitatively measured using an L&W brightness and brightness tester (Elrepho 070, Sweden). The tested items contained brightness and CIE L*a*b* values[36]. The micro-morphology variations of the recovered lignins were observed by field-emission scanning electron microscopy (FE-SEM, S-3400N II, HITACHI Company, Japan). Prior to the test, the lignins were taped onto electronic conductive tape and sprayed with gold. The average size (Z-ave) and size distribution of the LMPs were analyzed using a Zetasizer (Nano ZS, Malvern Instruments, UK). Before the analysis, the lignin samples were homogeneously dispersed in water (1 g/L) by sonication for 10 min.

The molecular weight of the lignin was quantified by gel permeation chromatography (GPC, Agilent, USA). Before the test, lignin was acetylated using pyridine/acetic anhydride (1:1, v:v) by magnetic stirring for 24 h. The acetylated lignins were then THF-dissolved and analyzed by GPC using a UV detector at 260 nm. Lignin samples (~150 mg) for Two-dimensional ^{1}H-^{13}C (2D) Heteronuclear Single-Quantum Correlation (HSQC) Nuclear Magnetic Resonance (NMR) analysis was prepared by being dissolved in DMSO-d_6 (0.6 mL). For quantification of hydroxyl groups by ^{31}P NMR, ~20 mg of dried lignin was mixed with 0.4 mL anhydrous pyridine and deuterated chloroform (1.6:1, v/v) to form a solution in an NMR tube, then 0.15 a mixed solution containing an internal standard (cyclohexanol) and relaxation agent (chromium acetylacetonate) was introduced. Before the test, an excess phosphitylation reagent (~0.1 mL of 2-chloro-4, 4, 5, 5-tetramethyl-1, 3, 2-dioxaphospholane) was introduced to react with the solution. For $^{\text{the}}$ ^{19}F NMR test, lignin was first derivatized with 4-(trifluoromethyl) phenylhydrazine. Briefly, ~60 mg of lignin was weighed into a bottle, followed by the addition of 1 mL of DMF-water solvent (v:v, 1:1) containing 110 mg of 4-(trifluoromethyl) phenylhydrazine. After stirring for 24 h at RT in the dark, the lignin was precipitated by introducing 20 mL of hydrochloric acid (pH 2.0) and then frozen. Upon melting, the derivatized lignin was washed, recovered by centrifugation, and then vacuum-dried at 50 °C for 24 h. The dried samples were dissolved in 0.6 mL DMSO-d6 containing an internal standard (3-trifluoromethoxybenzoic acid, 10 mg mL-1) and external standard (hexafluorobenzene, 10 mg mL^{-1}). 2D HSQC NMR, ^{31}P NMR and ^{19}F were performed using a Bruker Ascend^{TM} 600 MHz spectrometer, and the detailed sample preparation procedures and acquisition parameters were obtained from previous publications[35,37,38].

Substrate Characterization. The compositions of the raw and recovered substrates were analyzed by two-stage acid hydrolysis using the NREL protocol[39]. The monosaccharides from the acid hydrolysis were quantified using HPLC.

Preparation of LMPs sunscreen samples and determination of sun protection factor (SPF) All the LMPs based sunscreens were prepared by blending the LMPs (1 -5 wt% addition) and pure cream with constant magnetic stirring[34]. For example, 1 wt% LMPs sunscreen was synthesized by mixing 0.01 g LMPs and 0.99 g cream at 200 rpm for 5 h in a dark room at RT. For SPF measurement, a transparent tape was attached to a clear quartz slide with a thickness of 2 mm, and the experimental area was 12.5 cm^2 using a 2 mg/cm^2 sunscreen loading, according to a previous publication[34]. Prior to the test, each sample was dried for 15 min in the dark. For each sunscreen cream, a minimum of six non-overlapping spots were selected for UV transmittance measurement by UV-8000 (METASH, China) per nm in the wavelength range of 290-400 nm in the transmittance mode (T). The SPF value was calculated using the following equation:

$$SPF = \sum_{290}^{400} E_\lambda S_\lambda \Big/ \sum_{290}^{400} E_\lambda S_\lambda T_\lambda$$

Where E_λ is the erythemal spectral effectiveness, S_λ the solar spectral irradiance, and T_λ the spectral transmittance of the sample.

Acknowledgement. This work was supported by the Fundamental Research Funds of CAF (CAFYBB2023QA006), National Natural Science Foundation of China (32371821, 32301546, 32271974), the Jiangsu Province Key Laboratory of Biomass Energy and Materials (JSBEM-S-202203, JSBEM-S-202004), and the Young Elite Scientist Sponsorship Program by CAST. The AJR efforts were supported by the University of Tennessee, Knoxville.

References

1. Bertella, S. & Luterbacher, J. S. Lignin Functionalization for the Production of Novel Materials. *Trends Chem.* **2**, 440–453 (2020).
2. Questell-Santiago, Y. M., Galkin, M. V., Barta, K. & Luterbacher, J. S. Stabilization strategies in biomass depolymerization using chemical functionalization. *Nat. Rev. Chem.* **4**, 311–330 (2020).
3. Leppänen, I. *et al.* Capturing colloidal nano- and microplastics with plant-based nanocellulose networks. *Nat. Commun.* **13**, (2022).
4. Ragauskas, A. J. *et al.* Lignin valorization: Improving lignin processing in the biorefinery. *Science.* **344**, 1246843 (2014).
5. Cai, C. *et al.* Extracting high β -O-4 content lignin and by-producing substrate susceptible to enzymatic hydrolysis by a green flow through process. *Chem. Eng. J.* **453**, (2023).
6. Thoresen, P. P., Matsakas, L., Rova, U. & Christakopoulos, P. Recent advances in organosolv fractionation: Towards biomass fractionation technology of the future. *Bioresour. Technol.* **306**, 123189 (2020).

7. Pan, Z. *et al.* Fractionation of light-colored lignin via lignin-first strategy and enhancement of cellulose saccharification towards biomass valorization. *Ind. Crop. Prod.* **186**, 115173 (2022).
8. Huang, C. *et al.* Bioresource Technology Facilitating enzymatic hydrolysis with a novel guaiacol-based deep eutectic solvent pretreatment. *Bioresour. Technol.* **326**, 124696 (2021).
9. Liang, Y. *et al.* Bioresource Technology Novel betaine-amino acid based natural deep eutectic solvents for enhancing the enzymatic hydrolysis of corncob. *Bioresour. Technol.* **310**, 123389 (2020).
10. Ci, Y. H. *et al.* New ternary deep eutectic solvents for effective wheat straw deconstruction into its high-value utilization under near-neutral conditions. *Green Chem.* **22**, 8713–8720 (2020).
11. Shen, X. *et al.* Facile fractionation of lignocelluloses by biomass-derived deep eutectic solvent (DES) pretreatment for cellulose enzymatic hydrolysis and lignin valorization. *Green Chem.* **21**, 275–283 (2019).
12. Wang, Y. *et al.* Investigation of a Lignin-Based Deep Eutectic Solvent Using p - Hydroxybenzoic Acid for Efficient Woody Biomass Conversion. *ACS Sustain. Chem. Eng.* **8**, 12542–12553 (2020).
13. Liu, Y. *et al.* Tunable and functional deep eutectic solvents for lignocellulose valorization. *Nat. Commun.* **12**, 5452 (2021).
14. Tran, M. H., Phan, D. & Lee, E. Y. Review on lignin modifications toward natural UV protection ingredient for lignin-based sunscreens. *Green Chem.* **23**, 4633–4646 (2021).
15. Zhang, A. *et al.* Preparation of Light-Colored Lignosulfonate Sunscreen Microcapsules with Strengthened UV-Blocking and Adhesion Performance. *ACS Sustain. Chem. Eng.* **10**, 9381–9388 (2022).
16. Zhang, H., Liu, X., Fu, S. & Chen, Y. Fabrication of Light-Colored Lignin Microspheres for Developing Natural Sunscreens with Favorable UV Absorbability and Staining Resistance. *Ind. Eng. Chem. Res.* **58**, 13858–13867 (2019).
17. Qian, Y., Deng, Y., Li, H. & Qiu, X. Reaction-free lignin whitening via a self-assembly of acetylated lignin. *Ind. Eng. Chem. Res.* **53**, 10024–10028 (2014).
18. Zhang, H., Chen, F., Liu, X. & Fu, S. Micromorphology Influence on the Color Performance of Lignin and Its Application in Guiding the Preparation of Light-colored Lignin Sunscreen. *ACS Sustain. Chem. Eng.* **6**, 12532–12540 (2018).
19. Xia, Q. *et al.* Multiple hydrogen bond coordination in three-constituent deep eutectic solvents enhances lignin fractionation from biomass. *Green Chem.* **20**, 2711–2721 (2018).
20. Xie, J., Chen, J., Cheng, Z., Zhu, S. & Xu, J. Pretreatment of pine lignocelluloses by recyclable deep eutectic solvent for elevated enzymatic saccharification and lignin nanoparticles extraction. *Carbohydr. Polym.* **269**, 118321 (2021).
21. Li, N. *et al.* Enhancing enzymatic digestibility of bamboo residues using a three-constituent deep eutectic solvent pretreatment. *Bioresour. Technol.* **346**, 126639 (2022).
22. Mota, T. R. *et al.* Bioresource Technology Design of experiments driven optimization of alkaline pretreatment and saccharification for sugarcane bagasse. *Bioresour. Technol.* **321**, 124499 (2021).
23. Zhao, L. *et al.* Advances in pretreatment of lignocellulosic biomass for bioenergy production: Challenges and perspectives. *Bioresour. Technol.* **343**, 126123 (2022).
24. Tolbert, A., Akinosho, H. & Khunsupat, R. Characterization and analysis of the molecular weight of lignin for biorefi ning studies. *Biofuels, Bioprod. Bioref.* **8**, 836–856 (2014).

25. Capanema, E., Balakshin, M., Katahira, R., Chang, H. M. & Jameel, H. How well do MWL and CEL preparations represent the whole hardwood lignin? *J. Wood Chem. Technol.* **35**, 17–26 (2014).
26. Amiri, M. T., Bertella, S., Questell-Santiago, Y. M. & Luterbacher, J. S. Establishing lignin structure-upgradeability relationships using quantitative ^{1}H-^{13}C heteronuclear single quantum coherence nuclear magnetic resonance (HSQC-NMR) spectroscopy. *Chem. Sci.* **10**, 8135–8142 (2019).
27. Lu, F. & Ralph, J. Solution-state NMR of lignocellulosic biomass. *J. Biobased Mater. Bioenergy* **5**, 169–180 (2011).
28. Karlsson, M., Romson, J., Elder, T., Emmer, Å. & Lawoko, M. Lignin Structure and Reactivity in the Organosolv Process Studied by NMR Spectroscopy, Mass Spectrometry, and Density Functional Theory. *Biomacromolecules* **24**, 2314–2326 (2023).
29. Yu, Y. *et al.* Tailored one-pot lignocellulose fractionation to maximize biorefinery toward versatile xylochemicals and nanomaterials. *Green Chem.* **24**, 3257–3268 (2022).
30. Ajao, O. *et al.* Quantification and variability analysis of lignin optical properties for colour-dependent industrial applications. *Molecules.* **23**, 377 (2018).
31. Loureiro, P. E. G., Fernandes, A. J. S., Furtado, F. P., Carvalho, M. G. V. S. & Evtuguin, D. V. UV-resonance Raman micro-spectroscopy to assess residual chromophores in cellulosic pulps. *J. Raman Spectrosc.* **42**, 1039–1045 (2011).
32. Luo, X. *et al.* Protection Strategies Enable Selective Conversion of Biomass. *Angew.Chem.Int.Ed.* **59**, 11704–11716 (2020).
33. Lancefield, C. S., Panovic, I., Deuss, P. J., Barta, K. & Westwood, N. J. Pre-treatment of lignocellulosic feedstocks using biorenewable alcohols: Towards complete biomass valorisation. *Green Chem.* **19**, 202–214 (2017).
34. Qian, Y., Qiu, X. & Zhu, S. Lignin: A nature-inspired sun blocker for broadspectrum Sunscreens. *Green Chem.* **17**, 320–324 (2015).
35. Cheng, J. *et al.* Effective biomass fractionation and lignin stabilization using a diol DES system. *Chem. Eng. J.* **443**, 136395 (2022).
36. Lee, S. C., Yoo, E., Lee, S. H. & Won, K. Preparation and application of light-colored lignin nanoparticles for broad-spectrum sunscreens. *Polymers.* **12**, 699 (2020).
37. Meng, X. *et al.* Determination of hydroxyl groups in biorefinery resources via quantitative ^{31}P NMR spectroscopy. *Nat. Protoc.* **14**, 2627–2647 (2019).
38. Tang, B., Chong, K., Ragauskas, A. J. & Evans, R. Quantitative Low-Field ^{19}F Nuclear Magnetic Resonance Analysis of Carbonyl Groups in Pyrolysis Oils. *ChemSusChem.* **16**, 1–8 (2023).
39. Sluiter, A. *et al.* Determination of structural carbohydrates and lignin in Biomass - NREL/TP-510-42618. *Lab. Anal. Proced.* 17 (2008).